Accuracy Assessment of Modern Classification Techniques for Automatic Feature Extraction from Very High Resolution Satellite Imagery

By

Prof. Dr. Ahmed A. Shaker   Prof. Dr. Mahmoud M. Hamed
Prof. Dr. Ali A. Elsagheer   Eng. Mahmoud S. Mahmoud
Shoubra Faculty of Engineering, Banha University

الملخص العربي:

أصبح استخدام صور الجيل الجديد من الأقمار الصناعية عالية الدقة وسيلة فعالة لإنتاج الخرائط ذات مقاييس الرسم الكبيرة حيث أن العديد من المعالم مثل المباني و الطرق و المساحات الخضراء يمكن استتتاجها من هذه الصور، ونظرا لأن الطرق اليدوية لاستتتاج هذه المعالم بطيئة ومكلفة كان لا بد من اللجوء الى الطرق الأوتوماتيكية لتحسين كفاءة إنتاج الخرائط من صور الأقمار الصناعية والهدف من هذا البحث هو وضع مخطط لعملية الاستنتاج الأوتوماتيكي للمعالم من صور الأقمار الصناعية عالية الدقة و قد تم استخدام خمسة عشر نموذج رياضي خاص بعملية التصنيف، ثم معالجة لصور المصنفة وتحويلها إلى خرائط رقمية خطية. ولإتمام العمل تم استخدام صور ملونة من القمر الصناعي IKONOS ذات قدرة تحليلية متر و مقارنة النتائج بخرائط مقياس رسم 1:5000 الخاصة ببيئة المساحة و قد تم إجراء تجربتين الأولى بستخدام صورة القمر الصناعي فقط كمدخل لعملية التصنيف بينما تم إجراء التجربة الثانية باستخدام صورة القمر الصناعي بالإضافة إلى نموذج إرتفاعات رقمي. و في كلتي الحالتين تم جدولة النتائج و تحليلها ووضع التوصيات المقترحة.

Abstract:

The new generation of Very High Resolution Satellite Imagery (VHRSI) offers a mapping potential for large scale maps. Many features like buildings, roads and green areas could be extracted. Manual techniques are fading away as they are inefficient and time consuming. Thus, increasing the automation process improve the efficiency of satellite topographic mapping.

This research tries to set up a work flow for automatic feature extraction from VHRSI. Fifteen classification techniques were applied. The one meter pan sharpened IKONOS imagery are used to extract features that were compared against the already existing 1/5,000 maps.

Two experiments were conducted. For the first case, the classification is carried using the satellite images only as an input for the classification process. While for the second case, the classification is carried using the satellite imagery plus a Digital Surface Model (DSM) as an additional layer for the classification process. The classified images are then processed through a series of image processing steps to produce the digital vector map. For both cases all results are tabulated, analyzed and recommendations are mentioned.

1. Introduction

Researches on automated feature extraction from remotely sensed data has been increased in recent years by increasing the use of geographic information systems (GIS), and the need for data acquisition and update the information for GIS. Feature extraction has been approached in many different ways by digital image processors. Some of the methods are quite complex and require the fusion of several data sources or different scale space images [1].

Feature extraction is still a fundamental computer vision operation. There are different methodologies for feature extraction such as image fusion for feature extraction [2], fuzzy-based approach [3], mathematical morphology [4], model based approach [5], dynamic programming [6] and multi-scale grouping and context [7].

This paper presents a simple and accurate method for automatic feature extraction using fifteen of the most recent classification techniques.

2. Study Area

The area of study is selected at Roxi Square in Cairo city, covers approximately four squares Km. It is a largely urban area that contains buildings, a network of main roads as will as minor roads and some green areas.

3. Data Sources

a) A one-meter spatial resolution and pansharpened image over the area of study were collected in April 17, 2005 by Space Imaging's IKONOS satellite and supplied in a TIFF digital format (figure 2).

b) A 1/5000 topographic map for the same area of study produced in 1978 from 1/15000 aerial photographs acquired in 1977. The map is updated from the satellite imagery to preserve the accuracy of the comparison process. The map is published by the Egyptian Survey Authority (ESA), using the Universal Transverse Mercator (UTM) projection.

c) A digital surface model (DSM) covers the same area of study is generated from aerial photographs of scale 1:10,000 acquired in 2000. The negatives had been scanned using the color photogrammetric scanner (DELTASCAN), then the photogrammetric work station (DELTA) is used to generate the model. Nearly 70,583 points had been digitized and grided to produce a (2mx2m) grid file, which is converted into a raster format and then the UTM/WGS-84 projection is added (figure 4).

4. Methodology

Feature extraction of the study area was done based on the above mentioned data and was implemented in several stages as follow (Figure 1):

- Image to map geographic registration.
- Training stage.
- Evaluation of signatures.
- Classification stage.
- Classification accuracy assessment.
- Post classification smoothing.
- Raster to vector conversion process.
- Generalization of vector data.
- Evaluation of the produced map against the existing map

5. Image to Map Georeferencing

Accuracy assessments of the results require accurate image to map geographic registeration. The process involved georeferencing of both the Ikonos satellite image and the vector map to the Universal Transverse Mercator projection (UTM) using ERDAS IMAGINE-9.0 software Nearly 15 points evenly distributed through the area of study and well defined on both the map and the image were selected (figure 5). Image coordinates of the 15 points were compared against the corresponding Map Reference Points (MRPs) (Table 1). After geo-referencing (following the transformation), resampling was performed to move each digital value to the new position of the new corrected image In this study, for resampling, bilinear interpolation was used which has better results than nearest neighborhood and has less modification than cubic convolution [8]. The Root Mean Square (RMS) error from the satellite modeling were 1.775 m and 1.673 m in E and N respectively and the total error were 2.439 m.

For East and North coordinates RMSE for the 15 points were calculated as follow:

$$RMSE\ (N_i) = \sqrt{\frac{\sum_{i=1}^{15} \Delta N_i^2}{n-1}} \quad \text{.................(1)}$$

Where: ? N_i: is the X Residual for GCP_i.

n: is the GCP number, which equal 15 in this case.

Similar formula is used for RMSE (E)

6. Creation of signatures:

The overall objective of the creation of signature process is to assemble a set of statistics that describe the spectral response pattern for each land cover type to be classified in the image [9]. The minimum number of pixels required for a signature is the number of bands plus one (N+1), which is the necessary condition for the covariance matrix to be positive definite [10]. Nearly 20 signatures, evenly distributed through the image were selected for each class (figure 6)

7. Evaluation of signatures:

The created signatures are compared as a box plot illustrating minimum and maximum reflectance's to detect signatures which are similar [11]. The box plot option shows completely separable minimum/maximum boxes (Figure 7).

8. Image classification:

Due to the limitation of the number of pages available by the paper only the classification tree analysis (CTA) technique is discussed in details her, while the details and the mathematical models of the other used fourteen techniques could be found in [9], [10], [11].

Classification Tree Analysis (CTA) is a non-parametric univariate technique for classifying remotely sensed data. Using training site data. CTA successively splits the data to form homogenous subsets resulting in a hierarchical tree of decision rules.

A decision tree is composed of the following elements:

- The Root: The starting point of the tree.
- The Internode: The connections between the root. all other internodes, and the leaves.
- The Leaf: A group of pixels that either belong to the same class or are assigned to a particular class.

Starting from the root and using the training site data, pixels will be split and assigned along a binary split rule. If the pixels split are from the same class, they will be combined to form a leaf. If the split contains pixels from different classes, an internode is assigned and the process of splitting continues. Three splitting algorithms: Entropy. Gain Ratio and Gini are employed her as follows.

8.1. Entropy

$$Entropy = -\sum_{j=1}^{k} \frac{freq(C_{j,s})}{|s|} \times \log_2\left(\frac{freq(C_{j,s})}{|s|}\right) \dots\dots\dots(2)$$

$|s|$: Number of pixels in group s.

$C_{j,s}$: Number of pixels of class j in group s

$$Entropy_{X(s)} = \frac{|s_i|}{|s|} \times Entropy_{(s_i)} \quad\text{............(3)}$$

$$Gain_{(X)} = Entropy_{(s)} - Entropy_{X(S)} \quad\text{............(4)}$$

Gain: the gain of a single classification X is defined as the entropy after classification X. Gain (X) tests the maximization of the information gain [12].

8.2. Gain Ratio

The entropy algorithm is given to oversplitting since every split can potentially contribute to information gain. The gain ratio algorithm attempts to overcome this potential bias through a normalization process. If we define the split information of (X) as:

$$Split\, info_{(x)} = -\sum_{i=1}^{n} \frac{|S_i|}{S} \times \log^2\left(\frac{|S_i|}{S}\right) \quad\text{............(5)}$$

Which represents the potential information generated by dividing S into n subsets, and then the information gain measures the information as:

$$Gain\, Ratio_{(X)} = Gain_{(X)} / split\, info_{(X)} \quad\text{............(6)}$$

Where the gain ratio tends to maximize the above ratio [13]

8.3. Gini

The Gini splitting rule is a measure of impurity at a given internode that is at a maximum when all pixels are equally distributed among all classes. In general, the Gini splitting rule attempts to find the largest homogenous category within the dataset and isolate it from the remainder of the data [14].

$$Gini_{(s)} = \sum_{i} freq(C_{j,s}) \times (1 - freq(C_{j,s})) \quad\text{............(7)}$$

(Figures 8, 9) shows the results of the Gini classification model, before and after applying the digital surface model (DSM).

9. Creating masks for the thematic data

Each classified image is then separated into its three components (buildings, roads and green areas), producing a masked binary image for each individual class by converting

the digital number of the wanted class to one, while the digital numbers of the unwanted classes are converted to zeros (figure 10. a, b, c left).

10. Classification accuracy assessment:

To evaluate the classified image, it has been compared against the 1:5000 maps. From this comparison an error matrix that tabulates the different land cover classes to which cells have been assigned. Output also includes an overall error measure (tables 2, 3).

11. Post classification smoothing:

After converting the masked thematic data of buildings, roads and green areas into binary images (0, 1), the smaller raster homogeneous regions are merged into larger neighboring homogeneous regions or deleted according to an arbitrary 1m distance and $10m^2$ area thresholds. Regions are retained if they are larger than the given area threshold and is adjacent to a larger homogeneous region by a distance larger than 1m. The result is 3 black and white images (buildings, roads and green areas) without noisy features and also without holes (figure 10. a, b, c right).

12. Vector Generalization:

The smoothed masks of buildings, roads and green areas are then converted from raster to vector automatically producing noised lines due to the pixel existence in the raster image (Figure 11). To overcome the problem of the noised lines, the produced vector file from the raster to vector conversion process is processed again through a generalization process. This process simplifies the shapes of buildings, roads and green areas to remove unnecessary or unwanted details, while maintaining their essential shape and size [15]. Based on an arbitrary simplification tolerance of 5m and a minimum area of $10m^2$, the boundaries of buildings are enhanced so that all near-90-degree angles become exactly 90 degrees. Any building or a group of connected buildings with a total area smaller than the Minimum area will be excluded (Figure 12).

13. Results and Analysis

- This paper introduces a new procedure for feature extraction from VHRSI through applying modern classification techniques (15 techniques). The 1m pansharpened Ikonos image is used. Figures 2 and 3 shows the satellite imagery and the original map, while figures 8 and 9 show the CTA classification results as an example.

- To evaluate the accuracy of the classification process, an accurate estimation of the classes is carried out from the original map and compared against the corresponding classes form the classified image with and without applying the DSM data into the classification process (table 2), (table 3).

- The digital surface model (DSM) was generated from aerial photographs of scale 1:10,000 due to the limitation of ALS (Airborne laser scanner) data on hand.

- Without applying the DSM data into the classification process, the minimum overall classification accuracy is (11.02%) for the K-means classifier, while the maximum overall classification accuracy is (93.84%) for the CTA Classification (Table 4).

- When applying the DSM data into the classification process, the minimum overall classification accuracy is (29.07%) for the K-means classifier, while the maximum overall classification accuracy is (96.63%) for the CTA Classification (Table 5).

- From figures 13, 14, 15 we can select the most suitable and accurate classification technique for extracting buildings, roads or green areas from the 1m pansharpened Ikonos images, even if we have an elevation data source or not.

- The most suitable and accurate classification technique for extracting buildings from the 1m pansharpened Ikonos images and with no Digital Surface Model was FISHER classification (99.01%), while Fuzzy Art Map (FAM) was the most suitable and accurate one (99.99%) after applying the Digital Surface Model.

- The most suitable and accurate classification technique for extracting roads from the 1m pansharpened Ikonos images and without applying the Digital Surface Model was FISHER classification (100%), while Classification Tree Analysis (CTA) was the most suitable and accurate one (99.13%) after applying the Digital Surface Model.

- The most suitable and accurate classification technique for extracting green areas from the 1m pansharpened Ikonos images and without applying the Digital Surface Model was Classification Tree Analysis (CTA) (79.96%), while Classification FISHER was the most suitable and accurate one (96.13%) after applying the Digital Surface Model.

-1081-

- A sample of buildings from the produced map is compared against the original one and the minimum and maximum differences of area were 0.582 m^2 and 6.517 m^2 respectively (table 6).

- A sample of roads from the produced map is compared against the original one and the minimum and maximum differences of road width were 1.093 m and 2.981 m respectively (table 7).

- A sample of green areas from the produced map is compared against the original one and the minimum and maximum differences of area were 0.997 m^2 and 2.672 m^2 respectively (table 8).

- A number of the detected buildings, roads and green areas from the produced map are compared against the original one and the detection percents were 98.555, 100, and 93.333 for buildings, roads and green areas respectively (table 10).

- The statistics, discussed above (tables 6, 7, 8, 9 and 10), show the suitability of the proposed work follow for producing large scale maps from VHRSI.

- Although the map was produced in 1978, while the satellite image was acquired in 2005, the study area is an urban area and nearly has no major changes during this period of time.

14. Conclusions

- Accuracy of feature extraction could be increased or decreased by applying an elevation data source (DSM data) into the classification process according to the used model. However, the percentage of improvement is different in each classification technique tables 4 and 5.

- Some classification models are not sensitive for applying the DSM data and nearly give the same results Figures 13, 14, 15.

- The most suitable classification technique for extracting Roads, building and green areas from the 1m pansharpened Ikonos images and without applying the Digital Surface Model are FISHER, FISHER and Classification Tree Analysis (CTA) Respectively.

- The most suitable classification technique for extracting Roads, building and green areas from the 1m pansharpened Ikonos images and after applying the Digital Surface Model are Fuzzy Art Map (FAM), Classification Tree Analysis (CTA) and FISHER Respectively.

- Classification tree analysis classifier gives the better overall accuracy before and after applying the DSM data.

14. REFERENCES

[1] Hinz, S. and Baumgartner, A., 2003: "Automatic Extraction of Urban Road Networks from Multi-View Aerial Imagery". ISPRS Journal of Photogrammetry and Remote Sensing 58/1-2. pp. 83-98.

[2] Pigeon, L., Solaiman, B., and Toutin, T., 2001: "Linear planimetric feature domains modelling for multi-sensors fusion in remote sensing". In: Proceedings of SPIE AeroSense - International Symposium on Aerospace/Defence Sensing, Simulation, and Controls, Orlando, Vol. 4051, 8 p.

[3] Agouris, P., Gyftakis, S., and Stefanidis, A., 1998: "Using a fuzzy supervisor for object extraction within an integrated geospatial environment". In: International Archives of Photogrammetry and Remote Sensing, Vol. 32, Part III/1, pp. 191-195.

[4] Zhang, C., Murai, S. and Baltsavias, E., 1999: "Road network detection by mathematical morphology". In: Proceedings of ISPRS Workshop on 3D Geospatial Data Production: Meeting Application Requirements, Paris, France, Pages: 185-200.

[5] Buckner, J., 1998:" Model based road extraction for the registration and interpretation of remote sensing data". In: International Archives of Photogrammetry and Remote Sensing, Stuttgart, Germany, Vol. 32, Part 4/1, pp. 85-90.

[6] Gruen, A. and Li, H., 1995: "Semi-automatic road extraction by dynamic programming", ISPRS Journal of Photogrammetry and Remote Sensing, 50(4), pp. 11-20.

[7] Mayer, H., Laptev, I., and Baumgartner, A., 1997: "Automatic extraction based on Multi-Scale modeling, context and snakes". In: International Archives of Photogrammetry and Remote Sensing, Vol. 32, Part 3-2W3, pp. 106-113.

[8] R. P'eteri and T. Ranchin, 2003: "Multiresolution snakes for urban road extraction from ikonos and quickbird images", in 23nd EARSeL Annual Symposium "Remote Sensing in Transition", Ghent, Belgium, 2-5 June 2003.

[9] Lillesand, T., and Kiefer, R., (2004): "Remote Sensing and Image Interpretation". Fourth Edition. John Willey & Sons, Inc., New York.

[10] Schowengerdt, R., (2001): "Models and Methods for Image Processing". Second Edition. ACADEMIC PRESS. San Diego.

[11] IDRISI, 2006: "Idrisi Andes Trainning Reference Manual". Clark University, Worcester, USA.

[12] R. P'eteri, I. Couloigner, and T. Ranchin, 2003: "How to assess quantitatively road extracted from high resolution imagery?", Photogrammetric Engineering & Remote Sensing, 2003.

[13] Miller, J. and J. Franklin, 2001: "modelling the distribution of four vegetation alliances using generalized linear models and classification trees with spatial dependence". Ecological Modeling, 157: 227-247.

[14] Zambon, M., R. Lawrence, A. Bunn, and S. Powell, 2006: "Effect of alternative splitting rules on image processing using classification tree analysis". Photogrammetric Engineering and Remote Sensing, 72(1): 25-30.

[15] Rafael C. Gonzales, Richard E. Woods and Steven L. Eddins, 2004: "Digital Image Processing using Matlab", Pearson Education, Inc.
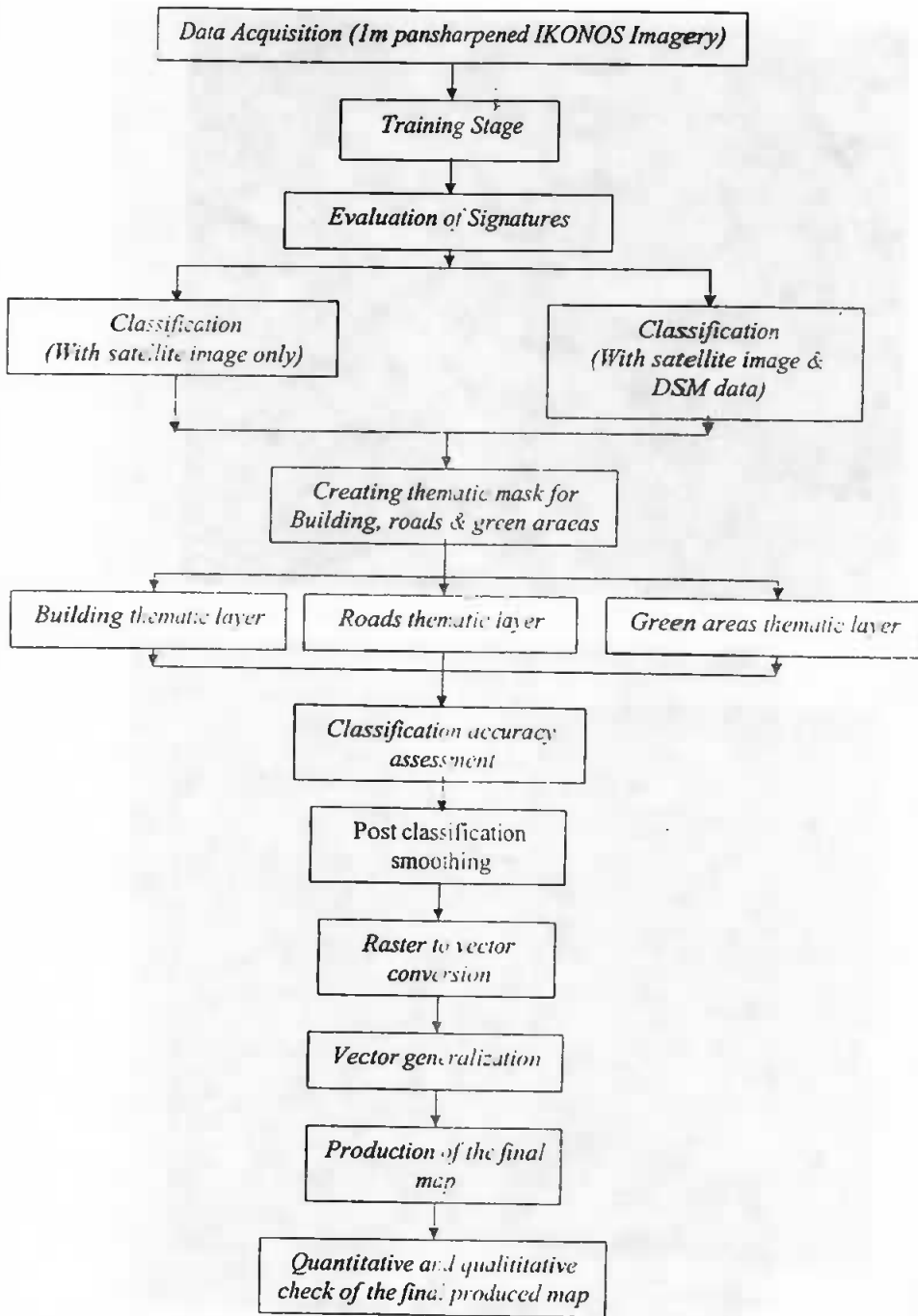
```
┌────────────────────────────────────────────────────────┐
│ Data Acquisition (1m pansharpened IKONOS Imagery)       │
└────────────────────────────────────────────────────────┘
                         │
                         ▼
              ┌─────────────────────┐
              │   Training Stage     │
              └─────────────────────┘
                         │
                         ▼
              ┌─────────────────────┐
              │ Evaluation of Signatures │
              └─────────────────────┘
              │                      │
              ▼                      ▼
┌──────────────────────┐   ┌──────────────────────┐
│   Classification      │   │   Classification      │
│ (With satellite image │   │ (With satellite image &│
│ only)                 │   │ DSM data)             │
└──────────────────────┘   └──────────────────────┘
              │                      │
              ▼                      ▼
              ┌─────────────────────┐
              │ Creating thematic mask for │
              │ Building, roads & green areas │
              └─────────────────────┘
       │              │              │
       ▼              ▼              ▼
┌───────────────┐ ┌───────────────┐ ┌───────────────────┐
│ Building      │ │ Roads         │ │ Green areas       │
│ thematic layer│ │ thematic layer│ │ thematic layer    │
└───────────────┘ └───────────────┘ └───────────────────┘
              │
              ▼
       ┌─────────────────────┐
       │ Classification accuracy │
       │ assessment           │
       └─────────────────────┘
              │
              ▼
       ┌─────────────────────┐
       │ Post classification  │
       │ smoothing            │
       └─────────────────────┘
              │
              ▼
       ┌─────────────────────┐
       │ Raster to vector     │
       │ conversion           │
       └─────────────────────┘
              │
              ▼
       ┌─────────────────────┐
       │ Vector generalization │
       └─────────────────────┘
              │
              ▼
       ┌─────────────────────┐
       │ Production of the final │
       │ map                  │
       └─────────────────────┘
              │
              ▼
       ┌─────────────────────┐
       │ Quantitative and qualititative │
       │ check of the final produced map │
       └─────────────────────┘
```

Figure (1): Steps of Automatic Features Extraction from VHRSI.

Figure (2): IKONOS Image of the Study Area.

Figure (3): The 1:5000 map of the Study Area.

Figure (4): The Generated Digital Surface Model (DSM).

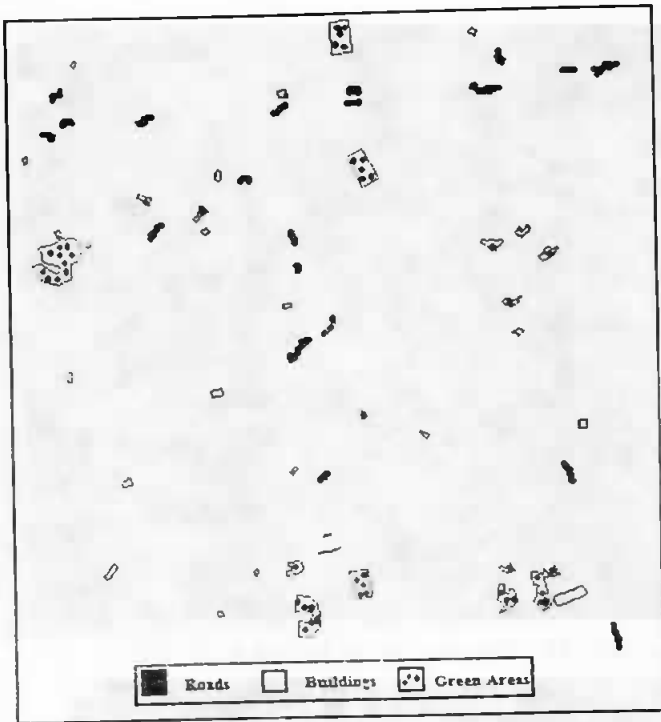Figure (5): Image Controls for Georeferencing Process.

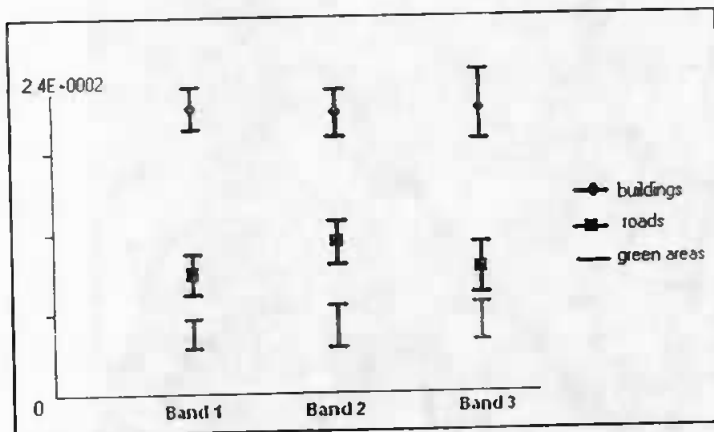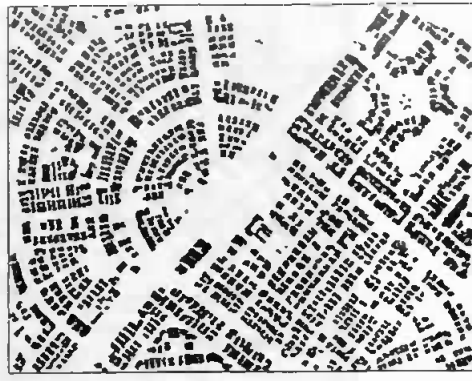*Figure (6): Buildings, Roads and Green areas signatures.*

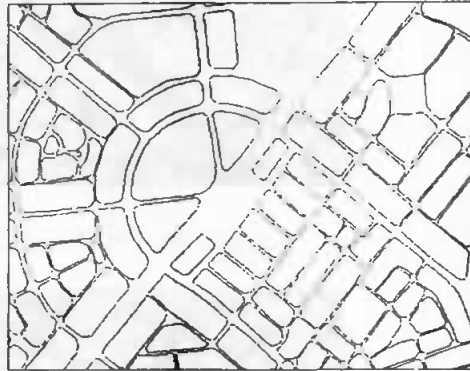*Figure (7): minimum and maximum reflectance's for Signatures.*

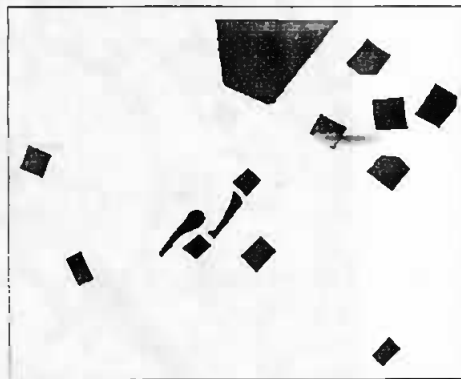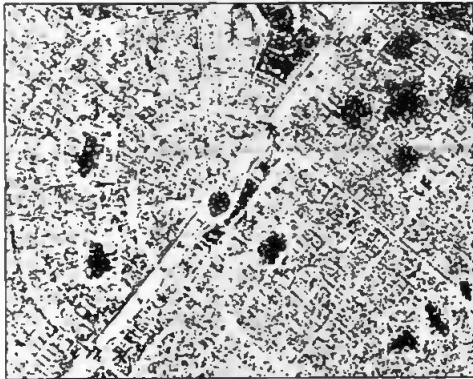*Figure (8): CTA Results before applying Elevation Data.*

Figure (9): CTA Results after applying Elevation Data.

(a): Buildings.

(b): Main Roads.

(c) Green Areas.

Figure (10): Buildings, roads and green areas masks before (left) and after (Right) smoothing and generalization.
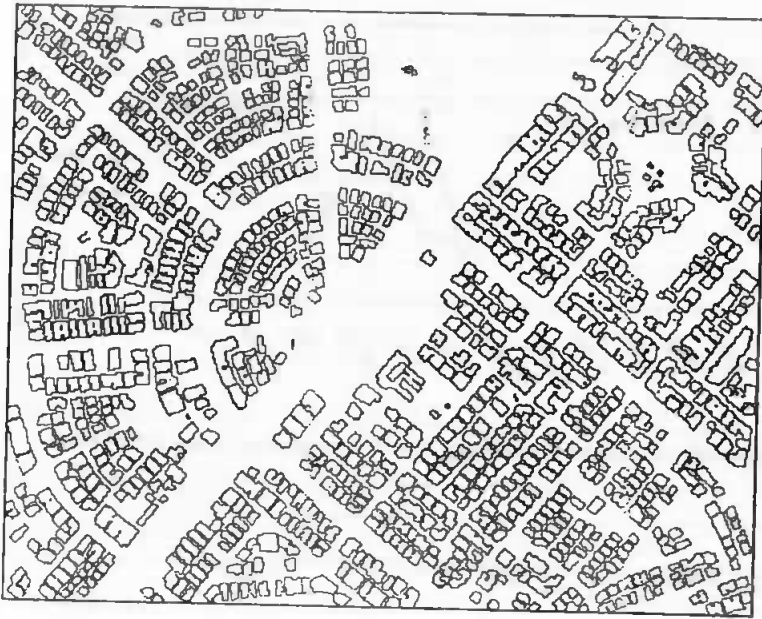
Figure (11): Buildings after Automatic Raster to Vector Conversion.
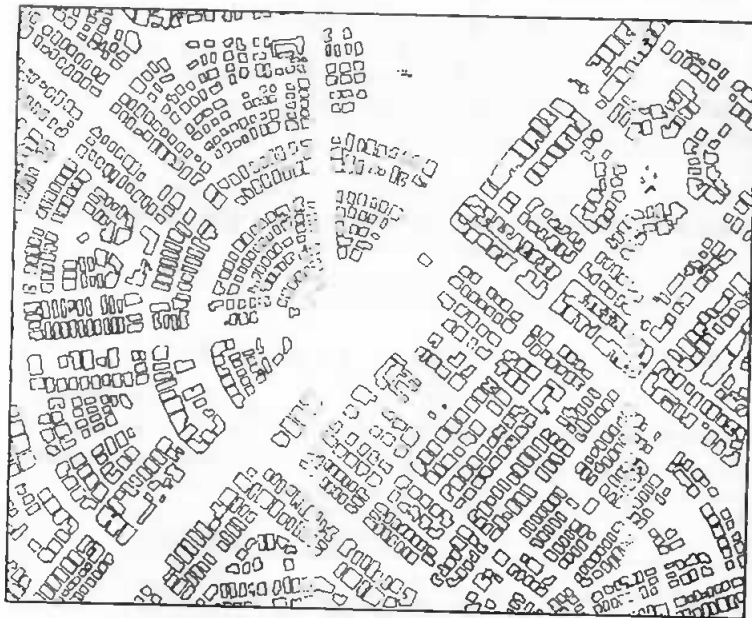

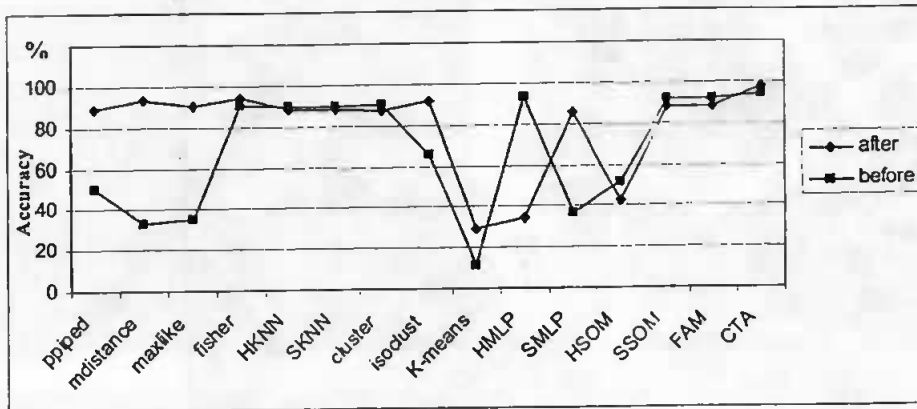*Figure (12): Buildings after Generalization Process.*

Figure (13): Overall classification accuracy before and after applying DSM Data.
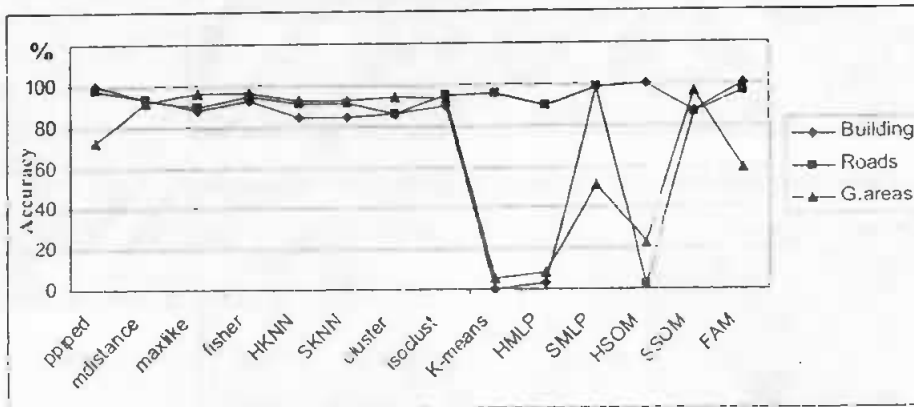

Figure (14): Building, Roads and G.areas classification accuracy after applying DSM Data.
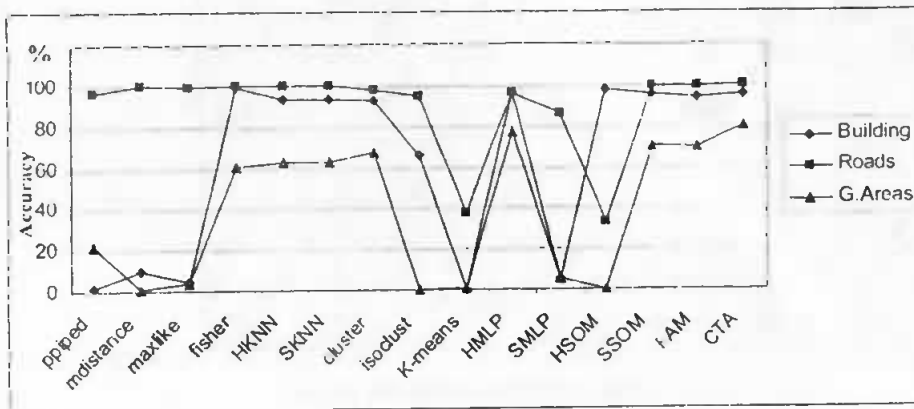

Figure (15): Building, Roads and G.areas classification accuracy before applying DSM Data.

Table (1): Accuracy of Image Georeferencing Using Map Coordinates

Pt.	X image (Meter)	Y image (Meter)	E MRPs (Meter)	N MRPs (Meter)	?E (Meter)	?N (Meter)	Result (Meter)
1	325685.344	3326935.040	325685.661	3326936.946	-1.910	-0.052	1.911
2	327613.535	3326902.534	327615.560	3326907.464	0.136	2.335	2.389
3	326969.833	3325514.507	326973.648	3325514.493	1.863	-1.688	2.514
4	325733.657	3325204.922	325737.533	3325206.264	1.770	0.202	1.781
5	326559.777	3326202.180	326562.875	3326205.518	1.050	1.460	1.798
6	326191.205	3326147.046	326193.059	3326147.633	-0.256	-1.148	1.176
7	326408.694	3325679.381	326410.052	3325681.311	-0.697	0.352	0.781
8	326765.684	3327118.327	326766.935	3327118.145	-0.744	-2.554	2.670
9	326130.651	3326632.394	326135.452	3326635.077	2.663	0.730	2.761
10	326922.337	3326489.892	326933.956	3326495.443	-0.344	3.418	3.435
11	326844.086	3325861.535	326845.728	3325862.719	-0.304	-0.618	0.688
12	325852.876	3325763.521	325854.810	3325764.553	-0.232	-0.414	0.474
13	325581.851	3326268.179	325583.451	3326271.044	-0.621	1.242	1.389
14	327385.361	3326156.811	327390.458	3326156.431	3.205	-2.493	4.060
15	326669.179	3326635.358	326669.918	3326635.460	-1.315	2.017	2.408

Table (2): Error Matrix Analysis of the classification tree analysis (CTA) classified image (rows) against the map (columns) before applying Elevation data source.

	Buildings	Roads	Green Areas	Total
Buildings	749313	0	10057	759370
Roads	3003	553943	89066	646012
Green areas	34191	1956	251227	251227
Total	786507	555899	314203	1656609

Overall Classification accuracy = 86.60 %

Table (3): Error Matrix Analysis of the classification tree analysis (CTA) classified image (rows) against the map (columns) after applying Elevation data source.

	Buildings	Roads	Green Areas	Total
Buildings	782092	43	17633	799768
Roads	0	551043	12327	563370
Green areas	4415	4813	284243	293471
Total	786507	555899	314203	1656609

Overall Classification accuracy = 96.20 %

Table (4): Accuracy Assessments of the classification Results before applying DSM Data.

No.	Classifier	Building accuracy	Roads accuracy	G. Areas accuracy	Overall accuracy %
1	ppiped	1.14	95.91	21.84	49.61
2	mdistance	9.80	99.89	0.99	33.05
3	maxlike	4.66	99.18	4.03	35.27
4	fisher	99.01	100.00	60.55	89.88
5	HKNN	93.38	99.82	62.46	89.31
6	SKNN	93.38	99.82	62.46	89.31
7	cluster	92.51	97.96	67.32	90.06
8	isoclust	65.41	94.71	0.00	65.27
9	K-means	0.00	37.41	0.77	11.02
10	HMLP	95.84	96.06	76.43	92.93
11	SMLP	5.04	85.91	4.86	36.55
12	HSOM	97.96	32.70	0.09	51.15
13	SSOM	95.60	99.36	69.72	91.97
14	FAM	94.02	99.21	69.64	91.44
15	CTA	95.27	99.65	79.96	93.84

Table (5): Accuracy Assessments of the classification Results after applying DSM Data.

No.	Classifier	Building accuracy	Roads accuracy	G. Areas accuracy	Overall accuracy %
1	ppiped	99.64	97.61	72.43	88.74
2	mdistance	93.53	93.24	91.48	92.91
3	maxlike	87.70	89.29	96.07	89.91
4	fisher	92.53	94.33	96.13	93.97
5	HKNN	84.55	91.28	92.47	88.24
6	SKNN	84.55	91.28	92.47	88.24
7	cluster	85.86	85.86	94.25	87.38
8	isoclust	89.61	94.46	92.96	91.90
9	K-means	0.11	95.73	5.45	29.07
10	HMLP	2.87	89.08	8.54	34.40
11	SMLP	98.73	98.40	50.81	85.93
12	HSOM	99.94	2.19	22.13	42.64
13	SSOM	86.35	85.88	95.79	87.89
14	FAM	99.99	96.15	58.73	87.72
15	CTA	99.44	99.13	90.40	97.63

Notes:
Ppiped: parallel piped. FISHER: Fisher classifier.
Mdistance: minimum distance. HKNN: Hard nearest neighbor.
Maxlike: maximum likelihood. SKNN: Soft nearest neighbor.
HMLP: Hard multilayer preceptor. CLUSTER: Cluster unsupervised.
SMLP: Soft multilayer preceptor. ISOCLUST: Iterative self-organizing unsupervised.
HSOM: Hard self organizing map. K-MEANS: K-means unsupervised
SSOM: Soft self organizing map.
FAM: Fuzzy art map classification.
CTA: classification tree analysis classification.

Table (6): Map versus Image Measurements of a Sample of Buildings using Classification Tree Analysis (CTA) models, in m².

No.	Map Area	Image Area		
		Gini model	Gain Ratio	Entropy
1	301.813	300.542	299.461	308.507
2	250.021	251.007	252.055	249.784
3	262.843	264.642	265.771	268.148
4	281.612	283.445	285.358	286.819
5	518.893	516.941	513.248	517.076
6	257.961	259.732	254.438	253.756
7	294.390	296.757	291.245	299.875
8	489.750	491.439	492.020	495.931
9	269.616	266.186	272.702	267.199
10	490.937	488.974	493.260	488.093

Table (7): Map versus Image Measurements of a Sample of Roads using Classification Tree Analysis (CTA) models, in m.

No.	Map Length	Image Length		
		Gini model	Gain Ratio	Entropy
1	722.7362	720.860	725.608	716.897
2	524.5510	525.644	528.453	528.943
3	587.6217	590.603	580.911	592.708
4	1448.2822	1449.378	1444.587	1443.614
5	512.0251	509.842	508.063	504.446

Table (8): Map versus Image Measurements of a Sample of Green Areas using Classification Tree Analysis (CTA) models, in m2.

No.	Map area	Image area		
		Gini model	Gain Ratio	Entropy
1	3558.529	3556.565	3560.201	3552.851
2	2114.026	2115.824	2116.755	2118.997
3	4575.645	4576.674	4578.882	4572.869
4	4492.501	4489.829	4485.513	4497.362
5	1371.568	1372.565	1368.272	1368.175

Table (9): Statistics of measurements differences of Buildings, Roads and green Areas using Classification Tree Analysis (CTA) models.

Feature	Min. Diff.	Max. Diff.	Mean Diff	RMS
Building areas	0.58751	6.516632	3.549192	
Road width	1.093	2.9813	2.03715	0.937
Green areas	0.997	2.672	1.8345	

Table (10): Map versus Image Quantitative differences of Buildings, Roads and green Areas using Classification Tree Analysis (CTA) models.

Feature	Source Map	Gini model	Detection Percent
No of Buildings	1246	1228	98.555
No of Roads	13	13	100
No of Green areas	15	14	93.333